Available online at www.sciencedirect.com
ScienceDirect
International Journal of Solids and Structures 44 (2007) 1256–1276
INTERNATIONAL JOURNAL OF SOLIDS and STRUCTURES
www.elsevier.com/locate/ijsolstr

Enhanced first-order theory based on mixed formulation and transverse normal effect

Jun-Sik Kim [a], Maenghyo Cho [b,*]

[a] Department of Aerospace Engineering, The Pennsylvania State University, University Park, PA 16802, USA
[b] School of Mechanical and Aerospace Engineering, Seoul National University, San 56-1, Shillim-Dong, Kwanak-Gu, Seoul 151-744, Republic of Korea

Received 25 January 2006; received in revised form 6 April 2006
Available online 20 June 2006

Abstract

An accurate prediction of displacements and stresses for laminated and sandwich plates is presented using an enhanced first-order plate theory based on the mixed variational theorem (EFSDTM) developed in this paper. In the mixed formulation, transverse shear stresses based on an efficient higher-order plate theory (EHOPT) developed by Cho and Parmerter [Cho, M., Parmerter, R.R., 1993. Efficient higher-order composite plate theory for general lamination configurations. AIAA Journal 31, 1299–1306] are utilized and modified to satisfy prescribed lateral conditions, and displacements are assumed to be those of a first-order shear deformation theory (FSDT). Relationships between the modified EHOPT and the FSDT are systematically derived via both the mixed variational theorem and the least-square approximation of difference between in-plane stresses including the transverse normal stress effect. It is shown that the transverse normal stress effect should be considered in predicting the in-plane stresses when the Poisson effect is dominant. The developed EFSDTM preserves the computational advantage of the classical FSDT while allowing for important local through-the-thickness variations of displacements and stresses through the recovery procedure. The accuracy and efficiency of the present theory are assessed by comparing its results with various plate models as well as the three-dimensional exact solutions for thick laminated and sandwich plates.

Keywords: Stress analysis; Plate theory; 3D stress recovery; Composite plates; Sandwich plates

1. Introduction

Numerous plate theories have been developed for the analysis of laminated and sandwich composite plates, because it is nowadays crucial to accurately and efficiently predict the behavior of composite plates providing excellent opportunities for light weight and high stiffness structures. It is a challenging problem to understand the behavior of laminated and sandwich plates with sufficient accuracy, especially for composite sandwich structures due to the strong shearing of a foam core. So far developed plate theories can be categorized into

* Corresponding author. Fax: +82 2 886 1693/883 1513.
E-mail address: mhcho@snu.ac.kr (M. Cho).

0020-7683/$ - see front matter © 2006 Published by Elsevier Ltd.
doi:10.1016/j.ijsolstr.2006.06.018

three classes, such as smeared theories (Lo et al., 1977; Kant, 1982; Reddy, 1984), zig-zag theories (DiSciuva, 1986; Cho and Parmerter, 1992), and layerwise theories (Reddy, 1987; Carrera, 1998). Comprehensive reviews and assessments in this field can be found in the survey papers by Noor and Burton (1989), Kapania and Raciti (1989), Reddy and Robbins Jr. (1994), and Carrera (2003). Plate theories based on the classical first-order shear deformation theory (FSDT) among others are briefly reviewed in the following.

The stress analysis in the design stage, various parametric studies should be followed. It is therefore desirable to develop a simple yet accurate stress prediction with a minimal number of degrees of freedom. The simplest shear deformation plate theory is a FSDT for isotropic plates proposed by Reissner (1945) and Mindlin (1951), which has been extended to laminated composites (Whitney and Pagano, 1970; Sun and Whitney, 1973). In the analysis of laminated composites, the FSDT is adequate to predict the global behavior. For high accuracy and fidelity of strength analysis, however, accurate prediction of stresses is required as well. There have been several efforts to improve the original FSDT, because it is still the most attractive approach due to its simplicity and low computational cost. One of them is to find the appropriate shear correction factors (SCFs) for laminated composites (Whitney, 1972, 1973). Noor and Burton (1990) proposed a predictor–corrector method for laminated and sandwich plates. The displacement fields have been calculated by integrating the equilibrium equation, in which the SCFs were obtained by an iterative manner in predictor phase, and through-the-thickness distributions were updated in corrector phase. A post-process method has been developed by Cho and Kim (1996a). An efficient higher-order plate theory (EHOPT) developed by Cho and Parmerter (1992, 1993) was utilized as a post-processor. They found the relationship between the FSDT with SCFs and an EHOPT under the assumption of the transverse shear energy equivalence. This method has been extended to general lamination configurations (Cho and Choi, 2001), various post-processors (Kim and Cho, 1998) and the finite element method (Cho and Kim, 1996b, 1997). Accuracy of both predictor–corrector and post-process methods strongly depends on the SCFs.

Several FSDT type plate theories have been developed by improving the transverse shear strains. Knight Jr. and Qi (1997) have developed a refined first-order shear deformation theory for laminated plates. They introduced the effective shear stress and strain so that the actual shear stress and strain are expressed in terms of the averaged shear strain of the original FSDT. An accurate asymptotically correct shear deformation theory was proposed by Sutyrin (1997). Yu et al. (2002) have, recently, developed a nonlinear "Reissner-like" plate theory based on the variational-asymptotic method. They have developed the computer program based on this, called variational-asymptotic plate and shell theory (VAPAS), by incorporating the one-dimensional through-the-thickness finite element analysis to overcome the analytical complexity of variational-asymptotic procedure (Yu et al., 2003). Recently, Yu (2005) extended this theory to allow maximum freedom for the asymptotically correct energy transformation. An enhanced first-order shear deformation theory (EFSDT) has been developed by Kim and Cho (2005), which was based on the definition of Reissner–Mindlin's plate theory. It was assumed that the displacement and in-plain strain fields of the FSDT can approximate those of three-dimensional theory in the averaged least-square sense. This theory has also been improved by minimizing the truncated strain energy (Kim, 2004; Kim and Cho, 2006). Icardi and Zardo (2005) proposed the strain energy updating method by utilizing the procedure to calculate the transverse normal stress in the FSDT developed by Rolfes et al. (1998).

Within this paper, an enhanced first-order shear deformation theory based on the mixed formulation (EFSDTM) is presented. A concept presented by the authors (Kim, 2004; Kim and Cho, 2005, 2006), which includes the displacement and stress recovery procedure, is extended to the mixed variational theorem (Reissner, 1950, 1986) to take the advantages of both FSDT and EHOPT. The explicit formulation for calculating the correction vector to in-plane displacements and strains is provided. With this, it will be shown that transverse stresses calculated by recovered displacements satisfy the lateral conditions at the top and bottom surfaces of the plates as well as the quasi three-dimensional equilibrium equations. The transverse normal stress effect cannot be ignored in predicting the in-plane stresses for some cases. In other words, the three-dimensional constitutive equations should be used in general. A comparison with the three-dimensional exact solutions and other available data in literature shows the accuracy and efficiency of the present theory.

2. Mixed formulation

A laminated plate of thickness h made of a monoclinic material is considered. Unless it is not differently specified, Greek indices will take values in the set 1, 2, whereas Latin indices will take values in 1, 2, 3. The

reference two-dimensional plane is represented by x_α and the through-the-thickness position is denoted by x_3, where $x_3 \in \left[-\frac{h}{2}, +\frac{h}{2}\right]$.

The three-dimensional constitutive equation is given by

$$\sigma_{ij} = C_{ijkl}\varepsilon_{kl}, \qquad \varepsilon_{kl} = \tfrac{1}{2}(u_{k,l} + u_{l,k}), \tag{1}$$

where σ_{ij}, ε_{kl} and u_i represent the stress tensor, strain tensor and displacements, respectively. C_{ijkl} denote the components of elasticity tensor with monoclinic symmetry properties. Subscripts $(\,)_{,i}$ denote partial derivatives with respect to x_i coordinates.

The Hellinger–Reissner functional (Reissner, 1950; Tarn and Wang, 1997) for the problem is expressed as

$$\Pi_R = \int_{-\frac{h}{2}}^{+\frac{h}{2}} \int_\Omega \left[\sigma_{ij}\frac{1}{2}(u_{i,j} + u_{j,i}) - W_c(\sigma_{ij}) - \widetilde{B}_i u_i\right] \mathrm{d}\Omega\,\mathrm{d}x_3 - \int_{S_\sigma} \widetilde{T}_i u_i \,\mathrm{d}S_\sigma - \int_{S_u} (u_i - \tilde{u}_i) T_i \,\mathrm{d}S_u, \tag{2}$$

where Ω represents the reference plane, $\widetilde{B}_i$ are the body forces, S_σ and S_u denote the boundaries with prescribed tractions $\widetilde{T}_i$ and prescribed displacements $\tilde{u}_i$, respectively, and $W_c(\sigma_{ij})$ is the complementary energy density function such that $\varepsilon_{ij} = \partial W_c/\partial\sigma_{ij}$,

$$\varepsilon_{\alpha\beta} = \partial W_c/\partial\sigma_{\alpha\beta} = \tfrac{1}{2}(u_{\alpha,\beta} + u_{\beta,\alpha}), \tag{3}$$

$$\varepsilon_{\alpha 3} = \partial W_c/\partial\sigma_{\alpha 3} = \tfrac{1}{2}S_{\alpha 3\beta 3}\sigma_{\beta 3} \equiv \varepsilon^*_{\alpha 3} = \tfrac{1}{2}\gamma^*_{\alpha 3}, \tag{4}$$

$$\varepsilon_{33} = \partial W_c/\partial\sigma_{33} = \frac{1}{C_{3333}}(\sigma_{33} - C_{33\alpha\beta}\varepsilon_{\alpha\beta}) \equiv \varepsilon^*_{33}, \tag{5}$$

in which $S_{\alpha 3\beta 3} = C^{-1}_{\alpha 3\beta 3}$. Henceforth ε_{ij} represents the strain tensor based on the displacements u_i, while ε^*_{i3} denotes the transverse strains derived from W_c.

The strains and in-plane stresses can be expressed in terms of u_i and σ_{i3} (Tarn and Wang, 1997), so that the displacements u_i and transverse stresses σ_{i3} are taken to be the functions subject to variations. Substituting Eqs. (1) and (3)–(5) into Eq. (2) yields

$$\begin{aligned}\delta\Pi_R = &\int_{-\frac{h}{2}}^{+\frac{h}{2}} \int_\Omega \left[(\sigma_{ij}\delta\varepsilon_{ij} + \gamma_{\alpha 3}\delta\sigma_{\alpha 3} + \varepsilon_{33}\delta\sigma_{33}) - \underline{(\gamma^*_{\alpha 3}\delta\sigma_{\alpha 3} + \varepsilon^*_{33}\delta\sigma_{33})} - \widetilde{B}_i\delta u_i\right] \mathrm{d}\Omega\,\mathrm{d}x_3 \\ &- \int_{S_\sigma} (\widetilde{T}_\alpha\delta u_\alpha + \widetilde{T}_3\delta u_3)\,\mathrm{d}S_\sigma - \int_{S_u} (u_i - \tilde{u}_i)\delta T_i \,\mathrm{d}S_u = 0,\end{aligned} \tag{6}$$

where the first terms come from $\sigma_{ij}\varepsilon_{ij}$ and the underline terms from W_c, which becomes

$$\begin{aligned}\delta\Pi_R = &\int_{-\frac{h}{2}}^{+\frac{h}{2}} \int_\Omega \left[\sigma_{\alpha\beta}\delta\varepsilon_{\alpha\beta} + \sigma_{\alpha 3}\delta\gamma_{\alpha 3} + \sigma_{33}\delta\varepsilon_{33} + \left(\gamma_{\alpha 3} - \gamma^*_{\alpha 3}\right)\delta\sigma_{\alpha 3} + \left(\varepsilon_{33} - \varepsilon^*_{33}\right)\delta\sigma_{33} - \widetilde{B}_i\delta u_i\right] \mathrm{d}\Omega\,\mathrm{d}x_3 \\ &- \int_{S_\sigma} (\widetilde{T}_\alpha\delta u_\alpha + \widetilde{T}_3\delta u_3)\,\mathrm{d}S_\sigma - \int_{S_u} (u_i - \tilde{u}_i)\delta T_i \,\mathrm{d}S_u = 0,\end{aligned} \tag{7}$$

in which the in-plane stresses $\sigma_{\alpha\beta}$ can be expressed as

$$\sigma_{\alpha\beta} = \sigma^{2D}_{\alpha\beta} + \overline{C}_{\alpha\beta 33}\sigma_{33}, \qquad \sigma^{2D}_{\alpha\beta} = Q_{\alpha\beta\gamma\omega}\varepsilon_{\gamma\omega}, \tag{8}$$

where

$$Q_{\alpha\beta\gamma\omega} = C_{\alpha\beta\gamma\omega} - \frac{C_{\alpha\beta 33}C_{\gamma\omega 33}}{C_{3333}}, \qquad \overline{C}_{\alpha\beta 33} = \frac{C_{\alpha\beta 33}}{C_{3333}}. \tag{9}$$

The prescribed boundary can be decomposed into two portions as

$$\int_{S_\sigma = \Omega^\pm + \Gamma_\sigma} (\widetilde{T}_\alpha\delta u_\alpha + \widetilde{T}_3\delta u_3)\,\mathrm{d}S_\sigma = \int_{\Gamma_\sigma} \left(\widetilde{T}^v_\alpha\delta u_\alpha + \widetilde{T}^v_3\delta u_3\right)\mathrm{d}\Gamma_\sigma + \int_{\Omega^\pm} (\tau^\pm_\alpha\delta u_\alpha + q^\pm\delta u_3)\,\mathrm{d}\Omega, \tag{10}$$

where $\Omega^\pm$ denotes the top and bottom surfaces of the plate, and $(\,)^+ = (\,)|_{x_3=+\frac{h}{2}}$, $(\,)^- = (\,)|_{x_3=-\frac{h}{2}}$.

From Eqs. (7) and (10), the Euler–Lagrange equations can be obtained as

$$\gamma_{\alpha 3} = u_{3,\alpha} + u_{\alpha,3} = S_{\alpha 3 \beta 3}\sigma_{\beta 3}, \tag{11}$$

$$\varepsilon_{33} = u_{3,3} = \frac{1}{C_{3333}}(\sigma_{33} - C_{33\alpha\beta}\varepsilon_{\alpha\beta}), \tag{12}$$

$$\sigma_{33,3} = -\sigma_{\alpha 3,\alpha} - \widetilde{B}_3, \tag{13}$$

$$\sigma_{\alpha 3,3} = -\left(\sigma^{2D}_{\alpha\beta} + \overline{C}_{\alpha\beta 33}\sigma_{33}\right)_{,\beta} - \widetilde{B}_\alpha, \tag{14}$$

and the boundary conditions are

$$u_i = \tilde{u}_i \quad \text{on } S_u, \tag{15}$$

$$[\sigma_{\alpha 3}, \sigma_{33}] = [\pm\tau^{\pm}_{\alpha}, \pm q^{\pm}] \quad \text{on } \Omega^{\pm}, \tag{16}$$

$$[\sigma_{\alpha\beta}v_\beta, \sigma_{\alpha 3}v_\alpha] = [\widetilde{T}^{v}_{\alpha}, \widetilde{T}^{v}_{3}] \quad \text{on } \Gamma_\sigma, \tag{17}$$

where v_α denotes the direction cosine of the outward normal v to the boundary Γ_σ on x_α direction.

In fact, the Euler–Lagrange equations, from Eqs. (11)–(14), provide the post-processing relations that will be described in later section.

With the assumptions that the edge tractions, which are related to the boundary layer effect (Gregory and Wan, 1985) or the Saint-Venant's principle (Tarn and Wang, 1997), are zero ($\widetilde{T}^{v}_{i} = 0$), the body forces are zero ($\widetilde{B}_i = 0$), and the transverse normal stress σ_{33} is negligible, the first variation of Hellinger–Reissner functional presented in Eq. (2), can be rewritten by

$$\delta(\Pi_R|_{\sigma_{33}=0}) = \delta\Pi^{2D}_R \equiv \int_\Omega \delta\widehat{\Pi}^{2D}_R \, d\Omega = 0, \tag{18}$$

in which

$$\delta\widehat{\Pi}^{2D}_R = \left\langle \sigma^{2D}_{\alpha\beta}\delta\varepsilon_{\alpha\beta} + \sigma_{\alpha 3}\delta\gamma_{\alpha 3} + (\gamma_{\alpha 3} - \gamma^{*}_{\alpha 3})\delta\sigma_{\alpha 3} \right\rangle - \left(\tau^{+}_{\alpha}\delta u^{+}_{\alpha} + \tau^{-}_{\alpha}\delta u^{-}_{\alpha}\right) - \left(q^{+}\delta u^{+}_{3} + q^{-}\delta u^{-}_{3}\right), \tag{19}$$

where $\langle\cdot\rangle = \int_{-h/2}^{+h/2}(\cdot)\,dx_3$.

One of the merits using the mixed formulation is that the transverse normal stress calculated via the 3D equilibrium equation analytically satisfies the prescribed tractions at top and bottom surfaces. This will be shown in later section.

3. Transverse shear stresses based on an efficient higher-order zig-zag theory

In the previous section, two independent fields are assumed for both displacements u_i and transverse shear stresses $\sigma_{\alpha 3}$. In this section, the transverse shear stresses are derived based on an efficient higher-order zig-zag theory developed by Cho and Parmerter (1992, 1993), which are expressed in terms of two variables. This makes it possible to find the exact relationships between transverse shear strains from FSDT and EHOPT.

The displacement fields for the perfectly bonded layers can be determined by the requirements, such that the transverse shear stresses should satisfy the prescribed shear tractions on the top and bottom surfaces of the plates and should be continuous through the thickness. These conditions can be satisfied by superimposing a linear zig-zag displacement, with a different slope in each layer, on overall cubic varying fields.

One can start with the displacement field that includes a cubic varying displacement and a linear zig-zag displacement:

$$u_\alpha(x_i) = u^0_\alpha(x_\alpha) + \psi_\alpha(x_\alpha)x_3 + \xi_\alpha(x_\alpha)x^2_3 + \phi_\alpha(x_\alpha)x^3_3 + \sum_{k=1}^{N-1} S^{(k)}_\alpha(x_\alpha)(x_3 - x_{3(k)})H(x_3 - x_{3(k)}), \tag{20}$$

$$u_3(x_i) = u^0_3(x_\alpha), \tag{21}$$

where the superscript, $()^0$, represents the variable on the reference plate, N is the number of layers, and $H(x_3 - x_{3(k)})$ is the Heaviside unit step function.

For monoclinic layers, the transverse shear stresses depend only on the transverse shear strains. Thus the prescribed shear tractions can be written as

$$\gamma^{+}_{\alpha 3} = \psi_\alpha + u^0_{3,\alpha} + \xi_\alpha h + \frac{3h^2}{4}\phi_\alpha + \sum_{k=1}^{N-1} S^{(k)}_\alpha = S^{+}_{\alpha 3\beta 3}\tau^{+}_\beta, \tag{22}$$

$$\gamma^{-}_{\alpha 3} = \psi_\alpha + u^0_{3,\alpha} - \xi_\alpha h + \frac{3h^2}{4}\phi_\alpha = -S^{-}_{\alpha 3\beta 3}\tau^{-}_\beta, \tag{23}$$

which are satisfied by

$$\psi_\alpha + u^0_{3,\alpha} = -\frac{3h^2}{4}\phi_\alpha - \frac{1}{2}\sum_{k=1}^{N-1} S^{(k)}_\alpha + \frac{1}{2}\left(S^{+}_{\alpha 3\beta 3}\tau^{+}_\beta - S^{-}_{\alpha 3\beta 3}\tau^{-}_\beta\right), \tag{24}$$

$$\xi_\alpha = -\frac{1}{2h}\sum_{k=1}^{N-1} S^{(k)}_\alpha + \frac{1}{2h}\left(S^{+}_{\alpha 3\beta 3}\tau^{+}_\beta + S^{-}_{\alpha 3\beta 3}\tau^{-}_\beta\right). \tag{25}$$

The transverse shear strains are then given by

$$\gamma_{\alpha 3} = 3\left(x_3^2 - \frac{h^2}{4}\right)\phi_\alpha + \gamma^{+}_{\alpha 3}\left(\frac{1}{2} + \frac{x_3}{h}\right) + \gamma^{-}_{\alpha 3}\left(\frac{1}{2} - \frac{x_3}{h}\right) + \sum_{k=1}^{N-1} S^{(k)}_\alpha\left[-\frac{1}{2} - \frac{x_3}{h} + H(x_3 - x_{3(k)})\right], \tag{26}$$

where $S^{(k)}_\alpha$ represents the change in slope at each interface and depends on the transverse shear material properties. This can be calculated by applying the continuity conditions of transverse shear stresses.

$$\sigma^{(k)}_{\alpha 3}|_{x_3 = x_{3(k)}} = \sigma^{(k+1)}_{\alpha 3}|_{x_3 = x_{3(k)}} \quad (k = 1, 2, \ldots, N-1). \tag{27}$$

From the preceding equations, one can obtain $2(N-1)$ linear algebraic equations of $2(N-1)$ unknowns $S^{(k)}_\alpha$. By solving this, $S^{(k)}_\alpha$ is obtained by

$$S^{(k)}_\alpha = a^{(k)}_{\alpha\beta}\phi_\beta + b^{(k)}_{\alpha\beta}\gamma^{+}_{\beta 3} + c^{(k)}_{\alpha\beta}\gamma^{-}_{\beta 3}, \tag{28}$$

where the terms $a^{(k)}_{\alpha\beta}$, $b^{(k)}_{\alpha\beta}$, and $c^{(k)}_{\alpha\beta}$ are functions of the material properties only. The derivation of Eq. (28) is similar to that presented in Cho and Parmerter (1992).

The transverse shear strains are then obtained by substituting Eq. (28) into Eq. (26). These can be expressed by

$$\gamma_{\alpha 3} = \mathscr{A}_{\alpha\beta}\phi_\beta + \mathscr{B}_{\alpha\beta}\gamma^{+}_{\beta 3} + \mathscr{C}_{\alpha\beta}\gamma^{-}_{\beta 3}, \tag{29}$$

in which

$$\mathscr{A}_{\alpha\beta} = 3\left(x_3^2 - \frac{h^2}{4}\right)\delta_{\alpha\beta} + \sum_{k=1}^{N-1} a^{(k)}_{\alpha\beta}\left[-\frac{1}{2} - \frac{x_3}{h} + H(x_3 - x_{3(k)})\right], \tag{30}$$

$$\mathscr{B}_{\alpha\beta} = \left(\frac{1}{2} + \frac{x_3}{h}\right)\delta_{\alpha\beta} + \sum_{k=1}^{N-1} b^{(k)}_{\alpha\beta}\left[-\frac{1}{2} - \frac{x_3}{h} + H(x_3 - x_{3(k)})\right], \tag{31}$$

$$\mathscr{C}_{\alpha\beta} = \left(\frac{1}{2} - \frac{x_3}{h}\right)\delta_{\alpha\beta} + \sum_{k=1}^{N-1} c^{(k)}_{\alpha\beta}\left[-\frac{1}{2} - \frac{x_3}{h} + H(x_3 - x_{3(k)})\right], \tag{32}$$

where $\delta_{\alpha\beta}$ is the Kronecker delta function.

Thus the transverse shear stresses can be written as follows:

$$\sigma_{\alpha 3} = C_{\alpha 3\beta 3}\left(\mathscr{A}_{\beta\lambda}\phi_\lambda + \mathscr{B}_{\beta\lambda}\gamma^{+}_{\lambda 3} + \mathscr{C}_{\beta\lambda}\gamma^{-}_{\lambda 3}\right). \tag{33}$$

It can be shown that the transverse shear stresses derived in Eq. (33) satisfy the lateral boundary conditions, $\sigma^{\pm}_{\alpha 3} = \pm\tau^{\pm}_\alpha$, because of that

$$\mathscr{A}^{\pm}_{\beta\lambda} = \mathscr{B}^{-}_{\beta\lambda} = \mathscr{C}^{+}_{\beta\lambda} = 0, \qquad \mathscr{B}^{+}_{\beta\lambda} = \mathscr{C}^{-}_{\beta\lambda} = \delta_{\beta\lambda}. \tag{34}$$

4. Mixed-based enhanced first-order plate theory

In this section, an enhanced first-order shear deformation theory based on mixed formulation (EFSDTM) is derived based on the mixed variational approach described in earlier section. The equilibrium equations and boundary conditions are derived, and followed by the recovering relations to the three-dimensional displacements and stresses.

4.1. Equilibrium equations and boundary conditions

The assumed displacements used in the mixed variational formulation are the same as those of Reissner–Mindlin's plate theory (Reissner, 1945; Mindlin, 1951). The assumed displacements are

$$\bar{u}_\alpha(x_i) = \bar{u}^0_\alpha(x_\alpha) + \theta_\alpha(x_\alpha)x_3, \qquad \bar{u}_3(x_i) = \bar{u}^0_3(x_\alpha). \tag{35}$$

Now we have two required fields, the transverse shear stresses and displacements. Substituting Eqs. (33) and (35) into Eq. (19) yields

$$\delta\widehat{\Pi}^{2D}_R = \overline{N}_{\alpha\beta}\delta\bar{u}^0_{\alpha,\beta} + \overline{M}_{\alpha\beta}\delta\theta_{\alpha,\beta} + Q_\alpha\delta(\theta_\alpha + \bar{u}^0_{3,\alpha}) - \left(\tau^0_\alpha\delta\bar{u}^0_\alpha + \tau^\theta_\alpha\delta\theta_\alpha\right) - q^0\delta\bar{u}^0_3 = 0, \tag{36}$$

where

$$\tau^0_\alpha = \tau^+_\alpha + \tau^-_\alpha, \qquad \tau^\theta_\alpha = \frac{h}{2}\left(\tau^+_\alpha - \tau^-_\alpha\right), \qquad q^0 = q^+ + q^-, \tag{37}$$

$$\bar{\gamma}_{\alpha3} = \theta_\alpha + \bar{u}^0_{3,\alpha}, \qquad [\overline{N}_{\alpha\beta}, \overline{M}_{\alpha\beta}] = \langle\bar{\sigma}^{2D}_{\alpha\beta}[1, x_3]\rangle, \qquad Q_\alpha = \langle\sigma_{\alpha3}\rangle, \tag{38}$$

and the constraint equation to be zero is

$$\langle(\bar{\gamma}_{\alpha3} - S_{\alpha3\beta3}\sigma_{\beta3})\delta\sigma_{\alpha3}\rangle = 0, \tag{39}$$

where $\gamma_{\alpha3}$, which is based on the assumed displacements of Eq. (35), is denoted by $\bar{\gamma}_{\alpha3}$ to distinguish it from Eq. (29).

The transverse shear force Q_α presented in Eq. (38) can be expressed as

$$Q_\alpha = \widehat{A}_{\alpha3\beta3}\phi_\beta + \widehat{B}_{\alpha3\beta3}\gamma^+_{\alpha3} + \widehat{D}_{\alpha3\beta3}\gamma^-_{\beta3}, \tag{40}$$

in which

$$[\widehat{A}_{\alpha3\beta3}, \widehat{B}_{\alpha3\beta3}, \widehat{D}_{\alpha3\beta3}] = \langle C_{\alpha3\gamma3}[\mathscr{A}_{\gamma\beta}, \mathscr{B}_{\gamma\beta}, \mathscr{C}_{\gamma\beta}]\rangle. \tag{41}$$

From Eq. (39), one can find that the transverse shear stresses variables (ϕ_β) can be expressed in terms of the displacement variables ($\bar{\gamma}_{\alpha3}$) as follows:

$$\widehat{A}_{\lambda3\alpha3}\bar{\gamma}_{\alpha3} = \widetilde{A}_{\lambda3\beta3}\phi_\beta + \widetilde{B}_{\lambda3\beta3}\gamma^+_{\beta3} + \widetilde{D}_{\lambda3\beta3}\gamma^-_{\beta3}, \tag{42}$$

where

$$[\widetilde{A}_{\lambda3\beta3}, \widetilde{B}_{\lambda3\beta3}, \widetilde{D}_{\lambda3\beta3}] = \langle\mathscr{A}_{\lambda\alpha}C_{\alpha3\gamma3}[\mathscr{A}_{\gamma\beta}, \mathscr{B}_{\gamma\beta}, \mathscr{C}_{\gamma\beta}]\rangle, \tag{43}$$

which renders

$$\phi_\beta = \widetilde{A}^{-1}_{\beta3\lambda3}\left(\widehat{A}_{\lambda3\alpha3}\bar{\gamma}_{\alpha3} - \widetilde{B}_{\lambda3\alpha3}\gamma^+_{\alpha3} - \widetilde{D}_{\lambda3\alpha3}\gamma^-_{\alpha3}\right). \tag{44}$$

Substituting Eq. (44) into Eq. (40) yields

$$Q_\alpha = A^*_{\alpha3\beta3}\bar{\gamma}_{\beta3} + B^*_{\alpha3\beta3}\gamma^+_{\beta3} + D^*_{\alpha3\beta3}\gamma^-_{\beta3}, \tag{45}$$

where

$$A^*_{\alpha3\beta3} = \widehat{A}_{\alpha3\mu3}\widetilde{A}^{-1}_{\mu3\lambda3}\widehat{A}_{\lambda3\beta3}, \tag{46}$$

$$B^*_{\alpha3\beta3} = \widehat{B}_{\alpha3\beta3} - \widehat{A}_{\alpha3\mu3}\widetilde{A}^{-1}_{\mu3\lambda3}\widetilde{B}_{\lambda3\beta3}, \tag{47}$$

$$D^*_{\alpha3\beta3} = \widehat{D}_{\alpha3\beta3} - \widehat{A}_{\alpha3\mu3}\widetilde{A}^{-1}_{\mu3\lambda3}\widetilde{D}_{\lambda3\beta3}. \tag{48}$$

Using Eq. (45), one can rewrite the two-dimensional Hellinger–Reissner functional given in Eq. (36) as

$$\delta\widehat{\Pi}_R^{2D} = \overline{N}_{\alpha\beta}\delta\bar{u}^0_{\alpha,\beta} + \overline{M}_{\alpha\beta}\delta\theta_{\alpha,\beta} + Q^*_\alpha\delta\left(\theta_\alpha + \bar{u}^0_{3,\alpha}\right) + Q^\tau_\alpha\delta\left(\theta_\alpha + \bar{u}^0_{3,\alpha}\right) - \left(\tau^0_\alpha\delta\bar{u}^0_\alpha + \tau^\theta_\alpha\delta\theta_\alpha\right) - q^0\delta\bar{u}^0_3 = 0, \tag{49}$$

where

$$Q^*_\alpha = A^*_{\alpha3\beta3}\bar{\gamma}_{\beta3}, \qquad Q^\tau_\alpha = B^*_{\alpha3\beta3}\gamma^+_{\beta3} + D^*_{\alpha3\beta3}\gamma^-_{\beta3}. \tag{50}$$

From Eq. (49), the governing equations for the present mixed-based enhanced first-order shear deformation theory are given by

$$\delta\bar{u}^0_\alpha : \overline{N}_{\alpha\beta,\beta} = -\tau^0_\alpha, \tag{51}$$

$$\delta\theta_\alpha : \overline{M}_{\alpha\beta,\beta} - \left(Q^*_\alpha + Q^\tau_\alpha\right) = -\tau^\theta_\alpha, \tag{52}$$

$$\delta\bar{u}^0_3 : Q^*_{\alpha,\alpha} + Q^\tau_{\alpha,\alpha} = -q^0, \tag{53}$$

and the associated boundary conditions are

$$\begin{aligned} &\delta\bar{u}^0_\alpha = 0 \quad \text{or} \quad \overline{N}_{\alpha\beta}v_\beta = 0,\\ &\delta\theta_\alpha = 0 \quad \text{or} \quad \overline{M}_{\alpha\beta}v_\beta = 0,\\ &\delta\bar{u}^0_3 = 0 \quad \text{or} \quad \left(Q^*_\alpha + Q^\tau_\alpha\right)v_\alpha = 0. \end{aligned} \tag{54}$$

Note that additional shear forces Q^τ_α are the prescribed quantities. In fact, these act like the external loading as shown in Eqs. (52) and (53).

4.2. Recovering relations

It is important to accurately predict the through-the-thickness stresses. Higher-order zig-zag theories presented in the previous section can be used as the post-processor to improve the prediction. This can be achieved by writing the displacement fields of the efficient higher-order zig-zag theory in terms of those of the present theory.

4.2.1. In-plane displacements

From Eqs. (20) and (29), the higher-order zig-zag displacement fields, which are compatible with Eq. (11), are given by

$$u_\alpha = u^0_\alpha - u^0_{3,\alpha}x_3 + \Phi_{\alpha\beta}\phi_\beta + \Lambda^p_{\alpha\beta}\gamma^+_{\beta3} + \Lambda^m_{\alpha\beta}\gamma^-_{\beta3}, \qquad u_3 = u^0_3, \tag{55}$$

where

$$\begin{aligned} \Phi_{\alpha\beta} &= \left(x_3^3 - \frac{3h^2}{4}x_3\right)\delta_{\alpha\beta} + \sum_{k=1}^{N-1} a^{(k)}_{\alpha\beta}f^{(k)}(x_3),\\ \Lambda^p_{\alpha\beta} &= \left(\frac{x_3}{2} + \frac{x_3^2}{2h}\right)\delta_{\alpha\beta} + \sum_{k=1}^{N-1} b^{(k)}_{\alpha\beta}f^{(k)}(x_3),\\ \Lambda^m_{\alpha\beta} &= \left(\frac{x_3}{2} - \frac{x_3^2}{2h}\right)\delta_{\alpha\beta} + \sum_{k=1}^{N-1} c^{(k)}_{\alpha\beta}f^{(k)}(x_3), \end{aligned} \tag{56}$$

in which

$$f^{(k)}(x_3) = \left[-\frac{x_3}{h} - \frac{x_3^2}{2h} + (x_3 - x_{3(k)})H(x_3 - x_{3(k)})\right]. \tag{57}$$

The definition of the mean displacement through the thickness of the plate (Reissner, 1950) is given by

$$\bar{u}^0_i = \frac{1}{h}\langle u_i\rangle, \tag{58}$$

which leads to the kinematical constraints on the displacements given as

$$u_\alpha^0 = \bar{u}_\alpha^0 - \frac{1}{h}\left(\langle \Phi_{\alpha\beta}\rangle \phi_\beta + \langle \Lambda_{\alpha\beta}^p\rangle \gamma_{\beta 3}^+ + \frac{1}{h}\langle \Lambda_{\alpha\beta}^m\rangle \gamma_{\beta 3}^-\right) - c_\alpha, \qquad u_3^0 = \bar{u}_3^0, \tag{59}$$

where c_α represent arbitrary functions of x_α introduced to satisfy the in-plane equilibrium equations, which accounts for the correction to symmetrical warping functions (Kim, 2004; Yu, 2005).

Using Eqs. (44), (55) and (59), one can recover the higher-order zig-zag displacement field as

$$u_\alpha = \bar{u}_\alpha^0 - \bar{u}_{3,\alpha}^0 x_3 + \Phi_{\alpha\beta}^* \bar{\gamma}_{\beta 3} + \Lambda_{\alpha\beta}^{p*}\gamma_{\beta 3}^+ + \Lambda_{\alpha\beta}^{m*}\gamma_{\beta 3}^- - c_\alpha, \tag{60}$$

where

$$\Phi_{\alpha\beta}^* = \left\{\Phi_{\alpha\lambda}(x_3) - \frac{1}{h}\langle \Phi_{\alpha\lambda}(x_3)\rangle\right\}\widetilde{A}_{\lambda 3\gamma 3}^{-1}\widehat{A}_{\gamma 3\beta 3}, \tag{61}$$

$$\Lambda_{\alpha\beta}^{p*} = \Lambda_{\alpha\beta}^p(x_3) - \frac{1}{h}\langle \Lambda_{\alpha\beta}^p(x_3)\rangle - \Phi_{\alpha\lambda}(x_3)\widetilde{A}_{\lambda 3\gamma 3}^{-1}\widetilde{B}_{\gamma 3\beta 3}, \tag{62}$$

$$\Lambda_{\alpha\beta}^{m*} = \Lambda_{\alpha\beta}^m(x_3) - \frac{1}{h}\langle \Lambda_{\alpha\beta}^m(x_3)\rangle - \Phi_{\alpha\lambda}(x_3)\widetilde{A}_{\lambda 3\gamma 3}^{-1}\widetilde{C}_{\gamma 3\beta 3}, \tag{63}$$

and $\bar{u}_i^0$ and $\bar{\gamma}_{\lambda 3}$ are obtained by solving Eqs. (51)–(53). The explicit form of c_α is given in Eq. (A.26) of Appendix A.

4.2.2. Stress recovery

To recover the three-dimensional stresses according to Eqs. (9), (13) and (14), the two-dimensional in-plane stresses and transverse normal stress should be calculated first.

The two-dimensional in-plane stresses are calculated by substituting Eq. (60) into Eq. (9). Then,

$$\sigma_{\alpha\beta}^{2\mathrm{D}} = Q_{\alpha\beta\gamma\omega}(u_{\gamma,\omega} + u_{\omega,\gamma})/2, \tag{64}$$

and the transverse normal stress using Eqs. (13) and (33) is obtained by

$$\sigma_{33}^{\mathrm{e}} = -\int_{-\frac{h}{2}}^{x_3} \sigma_{\alpha 3,\alpha}^{\mathrm{c}}\,\mathrm{d}x_3 - q^-, \tag{65}$$

where superscripts, $(\,)^{\mathrm{e}}$ and $(\,)^{\mathrm{c}}$, represent the quantities calculated via the equilibrium approach and constitutive one, respectively.

It can be shown that the transverse normal stress of Eq. (65) does satisfy the lateral boundary conditions ($\sigma_{33}^{\mathrm{e}\pm} = q^\pm$). From Eqs. (37) and (50), the transverse normal stress at top surface can be expressed as

$$\sigma_{33}^{\mathrm{e}+} = q^+ = -\langle \sigma_{\alpha 3}^{\mathrm{c}}\rangle_{,\alpha} - q^- = -(Q_{\alpha,\alpha}^* + Q_{\alpha,\alpha}^\tau) - q^-, \tag{66}$$

which becomes one of the governing equations, Eq. (53),

$$q^+ + q^- = q^0 = -(Q_{\alpha,\alpha}^* + Q_{\alpha,\alpha}^\tau). \tag{67}$$

With the transverse normal stress and two-dimensional in-plane stresses obtained, the three-dimensional in-plane stresses are then calculated as

$$\sigma_{\alpha\beta} = \sigma_{\alpha\beta}^{2\mathrm{D}}(\tilde{c}) + \overline{C}_{\alpha\beta 33}\sigma_{33}^{\mathrm{e}}, \tag{68}$$

where

$$\tilde{c} = \lfloor\, c_{1,1} \quad c_{2,2} \quad (c_{1,2} + c_{2,1})\,\rfloor^{\mathrm{T}}, \tag{69}$$

which is the correction vector that can be predetermined for any strain fields by using the least-square approximation of difference between in-plane stresses (Kim, 2004; Kim and Cho, 2006). This can be expressed by

$$\left\langle \min_{\bar{\sigma}_{\alpha\beta}^0} \|\sigma_{\alpha\beta}(\tilde{c}) - \bar{\sigma}_{\alpha\beta}^{2\mathrm{D}}\|_2^2 \right\rangle = 0 \quad \rightarrow \quad N_{\alpha\beta}(\tilde{c}) - \overline{N}_{\alpha\beta} = 0, \tag{70}$$

where $\bar{\sigma}_{\alpha\beta}^{2\mathrm{D}}$ are obtained using the displacements of Eq. (35). The detailed derivation of $\tilde{c}$ is given in Appendix A.

The transverse shear stresses using Eqs. (14) and (68) can be calculated by

$$\sigma^{\mathrm{e}}_{\alpha 3} = -\int_{-\frac{h}{2}}^{x_3} \sigma_{\alpha\beta,\beta}\,\mathrm{d}x_3 - \tau^-_\alpha. \tag{71}$$

One can show that the preceding equations satisfy the lateral boundary conditions ($\sigma^{\mathrm{e}\pm}_{\alpha 3} = \tau^{\pm}_{\alpha}$). At the top surface, the transverse shear stresses are

$$\sigma^{\mathrm{e}+}_{\alpha 3} = \tau^+_\alpha = -\langle \sigma_{\alpha\beta,\beta}\rangle - \tau^-_\alpha = -N_{\alpha\beta,\beta} - \tau^-_\alpha, \tag{72}$$

and $N_{\alpha\beta} = \overline{N}_{\alpha\beta}$, thanks to Eq. (70). Then

$$\sigma^{\mathrm{e}+}_{\alpha 3} = -\overline{N}_{\alpha\beta,\beta} - \tau^-_\alpha = \tau^+_\alpha \;\rightarrow\; -\overline{N}_{\alpha\beta,\beta} = \tau^+_\alpha + \tau^-_\alpha = \tau^0_\alpha, \tag{73}$$

which is one of the governing equations presented in Eq. (51).

Through the equations presented in above, it is shown that the recovered transverse stresses, σ^{e}_{i3}, satisfy traction conditions on the top and bottom surfaces that are $\sigma^{\mathrm{e}\pm}_{\alpha 3} = \pm\tau^{\pm}_{\alpha}$ and $\sigma^{\mathrm{e}\pm}_{33} = \pm q^{\pm}$. Thus the recovered stresses satisfy the following quasi three-dimensional equilibrium equations.

$$\sigma_{\alpha\beta,\beta} + \sigma^{\mathrm{e}}_{\alpha 3,3} = 0, \tag{74}$$

$$\sigma^{\mathrm{c}}_{\alpha 3,\alpha} + \sigma^{\mathrm{e}}_{33,3} = 0. \tag{75}$$

In order to satisfy the three-dimensional equilibrium of stresses, $\sigma^{\mathrm{e}}_{\alpha 3}$ should be used instead of $\sigma^{\mathrm{c}}_{\alpha 3}$ in Eq. (75). This will obviously increase the accuracy of σ_{33} and makes it mathematically more reasonable. By doing so, however, the fourth order derivatives are required to calculate the consistent σ_{33}, which is not favorable in practice.

Thus displacements and stresses are completely recovered in terms of primary variables $(\bar{u}^0_i, \theta_\alpha)$ of EFSDTM. The flowchart of procedures to obtain the present EFSDTM from H-R functional and to recover displacements and stresses is presented in Fig. 1.

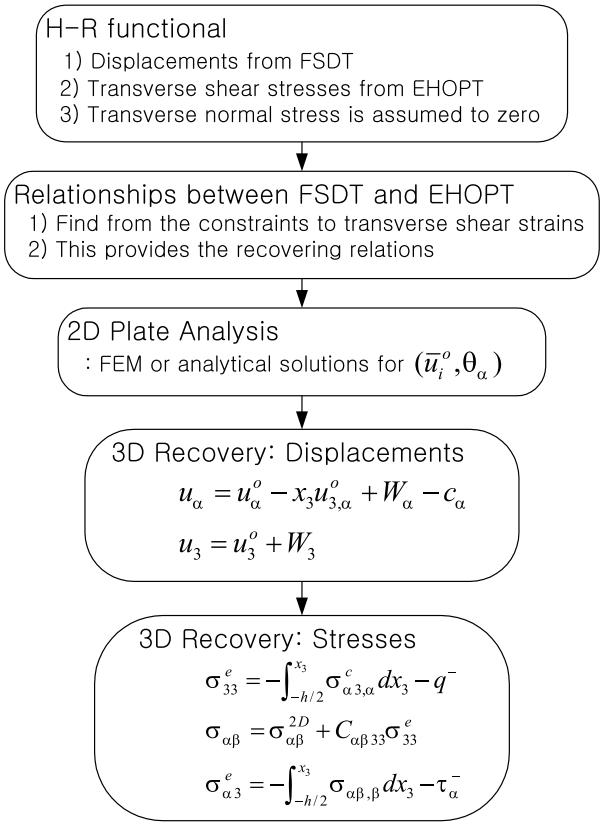

Fig. 1. Flowchart of procedure to obtain EFSDTM and recovery.

5. Numerical examples and discussion

In order to validate the present theory (EFSDTM), a number of laminated and sandwich plates are analyzed, and their results are compared to those of the three-dimensional elasticity. The exaction solutions of simply supported plates in cylindrical bending conditions developed by Pagano (1970) are reproduced and used as the benchmark solutions.

The ply material properties of all laminated plates are

$$\begin{aligned} &E_L = 172.4\ \text{GPa}, \qquad E_T = 6.9\ \text{GPa}, \\ &G_{LT} = 3.45\ \text{GPa}, \qquad G_{TT} = 1.38\ \text{GPa}, \qquad \nu_{LT} = \nu_{TT} = 0.25, \end{aligned} \tag{76}$$

where L denotes a fiber direction and T denotes a perpendicular direction to the fiber.

For sandwich plates, the material properties of face sheets are the same as Eq. (76), and the core material properties are taken as

$$\begin{aligned} &E_1 = 0.1\ \text{GPa}, \qquad G_{12} = 0.04\ \text{GPa}, \qquad \nu_{12} = 0.25, \\ &E_2 = E_3 = E_1, \qquad G_{23} = G_{13} = G_{12}, \qquad \nu_{23} = \nu_{13} = \nu_{12}. \end{aligned} \tag{77}$$

For all of the problems, a simply supported boundary condition is applied, the transverse load is assumed to have the form

$$q^{\pm} = \frac{p_0}{2} \sin\left(\frac{\pi x_1}{L_1}\right) \tag{78}$$

with $\tau_\alpha^{\pm} = 0$, and the displacements for these can be chosen to be of the form:

$$[\bar{u}_\alpha^0, \theta_\alpha] = [U_\alpha, \Theta_\alpha] \cos\left(\frac{\pi x_1}{L_1}\right), \tag{79}$$

$$\bar{u}_3^0 = U_3 \sin\left(\frac{\pi x_1}{L_1}\right). \tag{80}$$

The displacements and stresses reported herein are normalized by the following:

$$\hat{u}_\alpha = 100 E_T u_\alpha / p_0 h S^3, \qquad \hat{u}_3 = 100 E_T u_3 / p_0 h S^4, \qquad \hat{\sigma}_{ij} = \sigma_{ij}/p_0, \tag{81}$$

where S represents the length-to-thickness ratio defined by $S = L_1/h$.

The various models compared in the present study are listed in Table 1. A shear correction factor in the classical FSDT is assumed to be 5/6. In this study, the FSDT, HSDT and EFSDT results are reproduced. The transverse normal stress (σ_{33}^{e}) is calculated by integrating the three-dimensional equilibrium equations, in which transverse shear stresses ($\sigma_{\alpha 3}^{\mathrm{c}}$) are obtained through the constitutive equations, as shown in Eq. (65). The transverse shear stresses ($\sigma_{\alpha 3}^{\mathrm{e}}$), Eq. (71), are obtained from the equilibrium equations through integrating the in-plane stresses ($\sigma_{\alpha\beta,\beta}$).

Table 1
Shear deformation plate theories compared

Source	Theory	Degrees of freedom
Present	EFSDTM	5 (C^0,5)
Kim and Cho (2006)	EFSDT	5 (C^0,5)
Whitney and Pagano (1970)	FSDT	5 (C^0,5)
Yu (2005)	VAPAS	5 (C^0,5)
Cho and Parmerter (1993)	EHOPT	5 (C^1,7)
Pandya and Kant (1988)	HSDT	9 (C^0,9)
Carrera (1999a)	M1i, M3i	9 (C^0,9), 15 (C^0,15)
Lo et al. (1977)	LCW	11 (C^0,11)

5.1. Convergence and comparison of maximum deflections

The percentage errors of transverse deflections of the plate mid-plane as a function of the length-to-thickness ratio, S, are presented in Figs. 2 and 3 for laminated and sandwich plates. Fig. 2(a) shows an antisymmetric cross-ply laminated plate case, where the differences among FSDT, HSDT, EFSDT and EFSDTM are

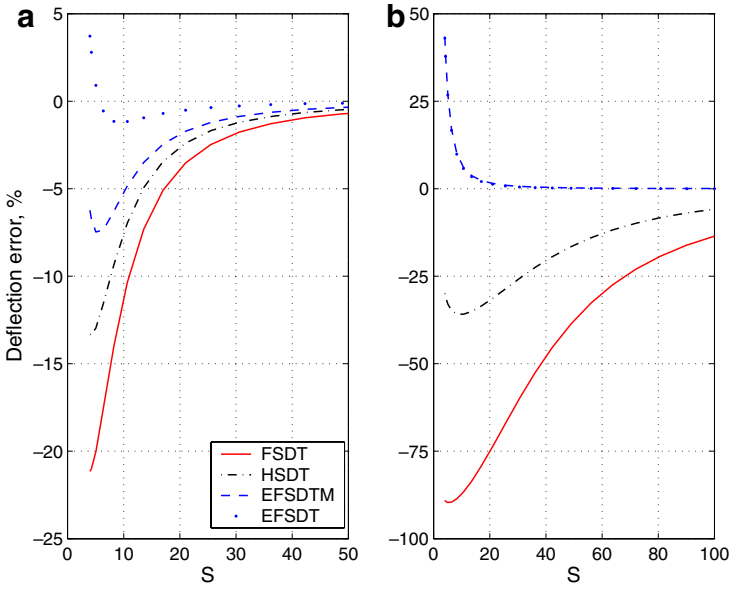

Fig. 2. Deflection errors of laminated and sandwich plates: (a) $[0.5°/90.5°]_2$ antisymmetric cross-ply plate, (b) [0.05°/Core(0.05°)/0.05°] sandwich plate.

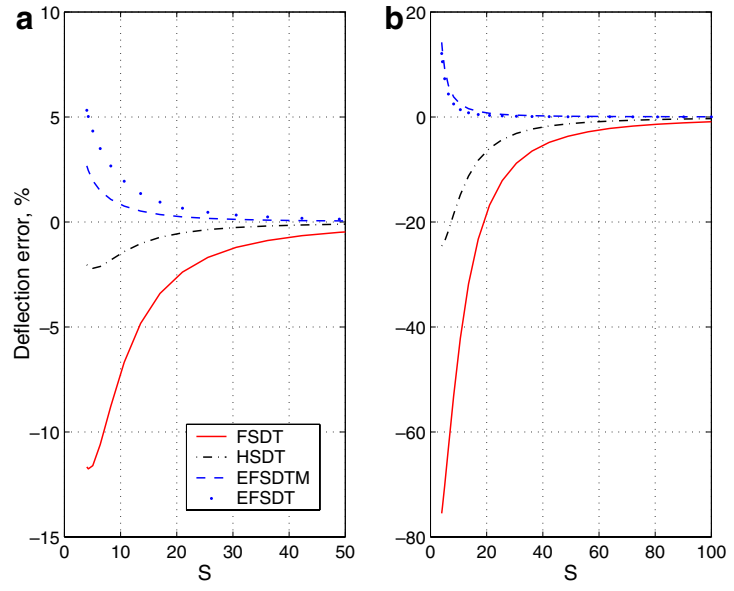

Fig. 3. Deflection errors of laminated and sandwich plates: (a) $[30°/-30°]_s$ symmetric angle-ply plate, (b) [−45°/Core(0.05°)/45°] sandwich plate.

small over $S > 50$ but rapidly grow the length-to-thickness ratio approaches $S = 4$. A sandwich plate is a very challenging problem because it experiences a significant shear deformation due to the flexible core material. Deflections predicted by the classical FSDT and HSDT are very poor, as shown in Fig. 2(b). Even for the very thin plate, $S = 100$, the percentage errors of FSDT and HSDT to the exact solution are -14% and -6%, respectively. While those of the EFSDT and present theory (EFSDTM) are less than 2% when $S \geqslant 20$. In

Table 2
Maximum normalized deflection $\hat{u}_3$ $(x_3 = 0)$ of symmetric and antisymmetric cross-ply plates

	[0°/90°/0°]				[0°/90°/0°/90°]			
	$S = 4$	$e\%$	$S = 6$	$e\%$	$S = 4$	$e\%$	$S = 6$	$e\%$
Exact	2.887	–	1.635	–	4.181	–	2.556	–
EFSDTM	3.273	13	1.738	6	3.920	−6	2.367	−7
EFSDT	3.226	12	1.717	5	4.336	4	2.552	−0
FSDT	2.409	−17	1.354	−17	3.296	−21	2.090	−18
EHOPT	–	–	–	–	4.083	−2	2.501	−2
M1i	2.904	−1	1.634	−0	3.300	−21	2.095	−18
M3i	2.881	−0	1.634	−0	4.102	−2	2.514	−2
HSDT	2.706	−6	1.520	−7	3.623	−13	2.251	−12
LCW	2.687	−7	1.514	−7	3.587	−14	2.242	−12

Table 3
Maximum normalized deflection $\hat{u}_3$ $(x_3 = 0)$ of symmetric and antisymmetric angle-ply plates

	$[30°/-30°]_s$				$[30°/-30°]_2$			
	$S = 4$	$e\%$	$S = 10$	$e\%$	$S = 4$	$e\%$	$S = 10$	$e\%$
Exact	3.290	–	1.285	–	3.291	–	1.385	–
EFSDTM	3.378	2.7	1.295	0.8	3.171	−3.6	1.346	−2.8
EFSDT	3.465	5.3	1.312	2.1	3.350	1.8	1.375	−0.7
FSDT	2.906	−11.7	1.192	−7.2	2.787	−15.3	1.285	−7.2
HSDT	3.223	−2.0	1.265	−1.6	2.941	−10.6	1.315	−5.1

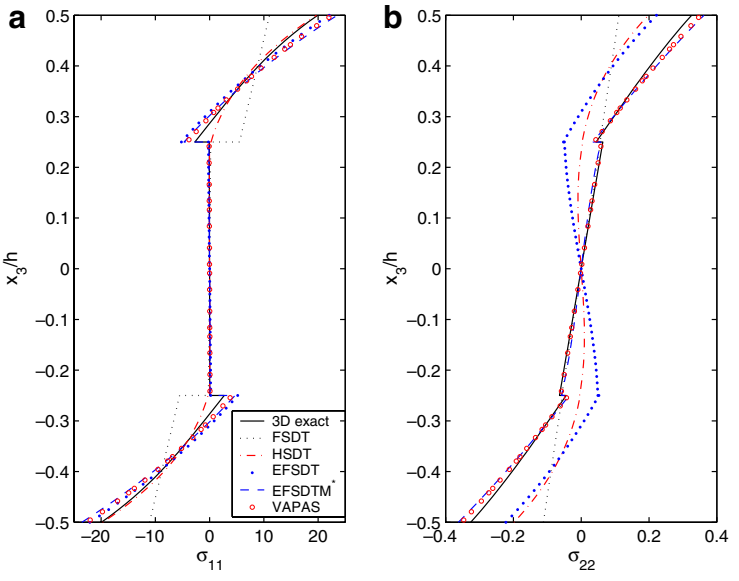

Fig. 4. In-plane stresses of a $[0.5°/90.5°]_s$ plate with $S = 4$: (a) $\hat{\sigma}_{11}$, (b) $\hat{\sigma}_{22}$.

Fig. 3, deflection errors of symmetric angle-ply laminated plate (a) and antisymmetric sandwich plate (b) are plotted. Similar deflection convergence patterns to Fig. 2 are observed. From Figs. 2(a) and 3(a), one can see that the present EFSDTM is more accurate than EFSDT for an angle-ply plate, while it is less accurate for a cross-ply plate.

Maximum normalized deflections of thick cross-ply plates are listed and compared to other available results in Table 2, where the plate is loaded at the top surface and the data are taken from Carrera (1999a). For symmetric and antisymmetric angle-ply plates, maximum normalized of deflections are listed in Table 3. The present theory and EFSDT gives the best compromised results in terms of accuracy, numerical efficiency and degrees of freedom (see Table 1) when both symmetric and antisymmetric laminated plates are considered. It is seen that EFSDTM yields less accurate results than EFSDT for antisymmetric lay-up cases. The good performance of EFSDT for such cases is achieved by sacrificing the accuracy of the transverse normal stress. This will be illustrated in later.

5.2. Transverse normal stress effect to in-plane stresses

Fig. 4 shows the normalized in-plane stresses of a symmetric nearly cross-ply plate, [0.5°/90.5°/90.5°/0.5°], for the very thick case of $S = 4$. A good agreement between the present EFSDTM and the three-dimensional

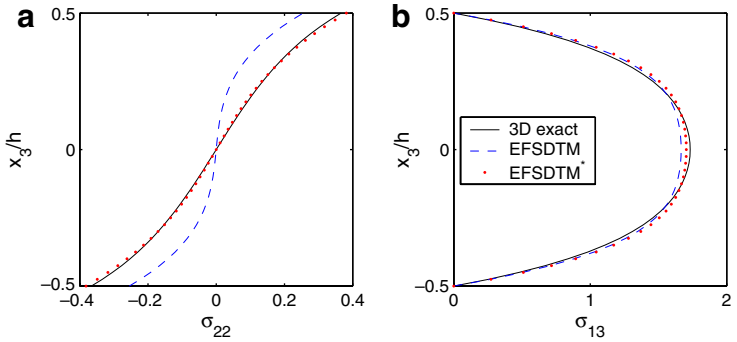

Fig. 5. Stresses of a single layered plate, [5°], with $S = 4$: (a) in-plane stress $\hat{\sigma}_{22}$, (b) transverse shear stress $\hat{\sigma}_{13}$.

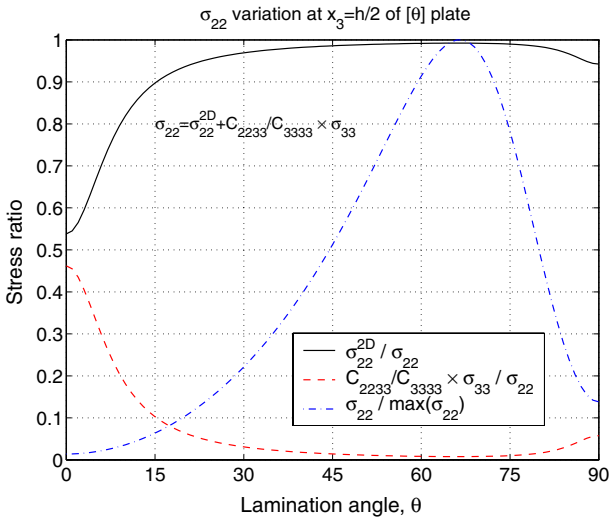

Fig. 6. In-plane stress ratio variations of a single layered plate, [θ°], with $S = 4$.

elasticity is found for the in-plane stress σ_{11}. As can be seen from Fig. 4, both the HSDT and EFSDT fail to give an accurate in-plane stress σ_{22}, whereas the VAPAS and EFSDTM* give comparable results to the exact solution since they utilized the three-dimensional constitutive equations. In other words, the transverse normal stress is considered in predicting the in-plane stresses. To verify this further, the in-plane stress σ_{22} and transverse normal stress σ_{33} of a single layered plate, [5°], are presented in Fig. 5 where the in-plane stress σ_{22} by EFSDTM* includes the transverse normal stress according to Eq. (68). The in-plane stress can be significantly improved by incorporating the transverse normal stress effect, while its effect to the transverse shear stresses is not significant. To identify the contributions of the 2D in-plane stress and transverse normal stress to the 3D in-plane stress, the stress ratio variations with the lamination angle $\theta°$ are depicted in Fig. 6. It can be concluded that the transverse normal stress to the in-plane stress is important when the in-plane stress is dominated by the Poisson effect.

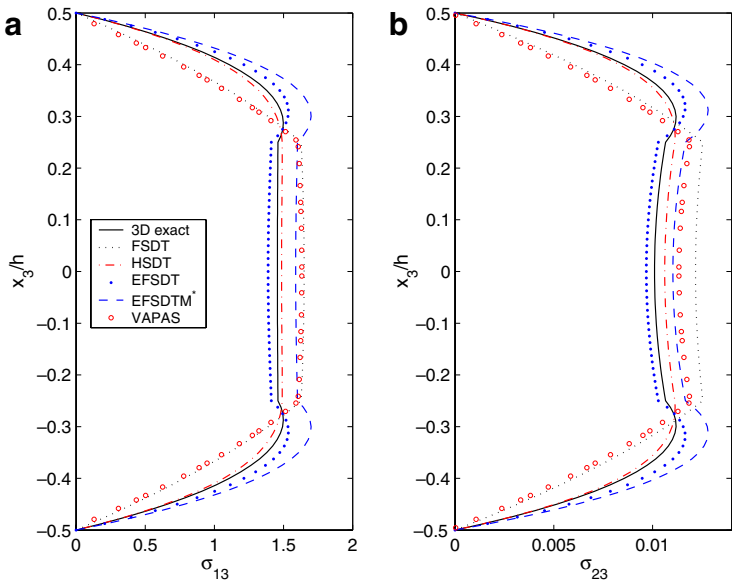

Fig. 7. Transverse shear stresses of a $[0.5°/90.5°]_s$ plate with $S = 4$: (a) $\hat{\sigma}_{13}$, (b) $\hat{\sigma}_{23}$.

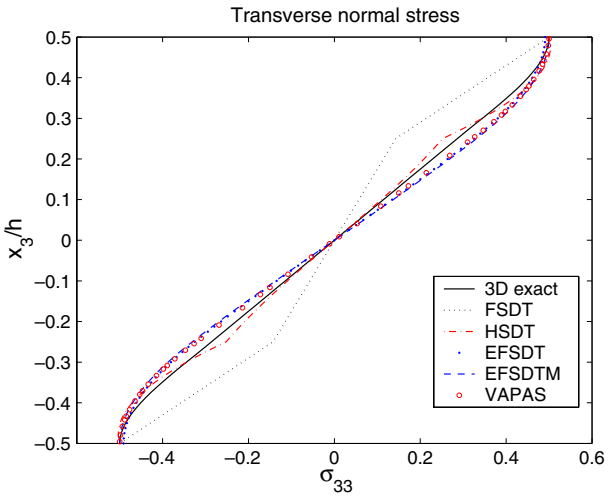

Fig. 8. Transverse normal stress $\hat{\sigma}_{33}$ of a $[0.5°/90.5°]_s$ plate with $S = 4$.

5.3. Through-the-thickness variations of displacements and stresses

Figs. 7 and 8 compare normalized transverse stresses of a $[0.5°/90.0°]_s$ symmetric cross-ply plate with $S = 4$. The kinky distributions of $\sigma_{\alpha 3}$ (Fig. 7) can be well captured by the EFSDT and present EFSDTM, while other theories, such as FSDT, HSDT and VAPAS, can not represent such a kinky shape. It is seen that the EFSDT is better than the EFSDTM in predicting the transverse shear stresses. The EFSDT, however, does not exactly satisfy the lateral conditions of transverse normal stress, $\sigma_{33}^{\pm} = \pm\frac{p_0}{2}$, as it is shown in Fig. 8. In order to compare the case of practical laminated plate, a symmetric angle-ply plate with $[30°/-30°/-30°/30°]_5$ and $S = 4$, an example taken from Yu (2005) is also considered. Transverse shear stresses for this case are reported in Fig. 9, where the present results are compared to those of FSDT, HSDT, VAPAS and 3D elasticity. The EFSDTM shows a good agreement with both the EFSDT and HSDT. Furthermore, the EFSDTM results

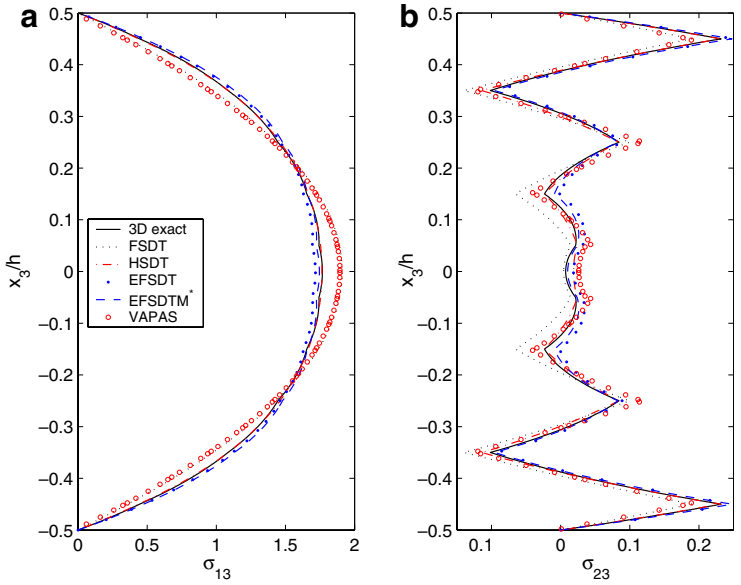

Fig. 9. Transverse shear stresses of a $[30°/-30°/-30°/30°]_5$ plate with $S = 4$: (a) $\hat{\sigma}_{13}$, (b) $\hat{\sigma}_{23}$.

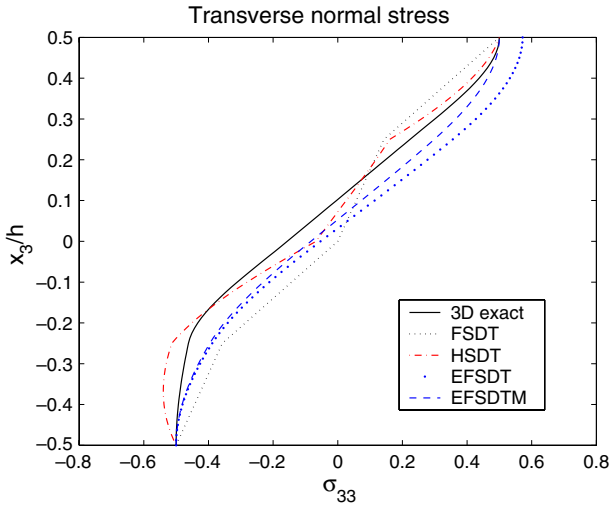

Fig. 10. Transverse normal stress $\hat{\sigma}_{33}$ of a $[0.5°/90.5°]_2$ plate with $S = 4$.

match the exact solutions with excellent accuracy. In Fig. 10, the transverse normal stress of an antisymmetric cross-ply plate with $S = 4$ is presented and compared to other models. As mentioned earlier, the deflection predicted by EFSDT is more accurate than the present EFSDTM. Such a good prediction of EFSDT needs the flexible transverse shear stiffness. This, however, leads to the overestimation of the transverse normal stress, as shown in Fig. 10. This confirms the superiority of the present theory in predicting the transverse normal stress compared to FSDT, HSDT and EFSDT. In fact, the layerwise model with 44 sub-laminates is required to precisely predict the transverse normal stress in this case (Icardi, 2001).

In order to demonstrate the accuracy of present theory in predicting the static behavior of sandwich plates showing a significant transverse shear deformation effect, a [0.05°/Core(0.05°)/0.05°] sandwich plate with the thickness of each face sheet that equals to $h/10$ is considered first. The in-plane displacement and transverse shear stresses for a thick sandwich plate of $S = 10$ are shown in Figs. 11 and 12, respectively. The present the-

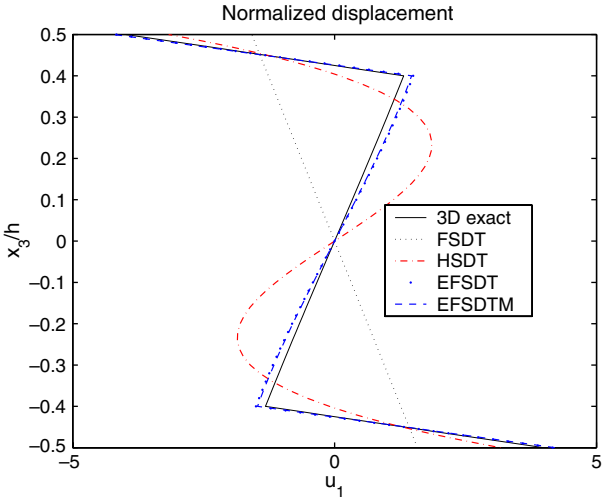

Fig. 11. In-plane displacement $\hat{u}_1$ of a [0.05°/Core(0.05°)/0.05°] sandwich plate with $S = 10$.

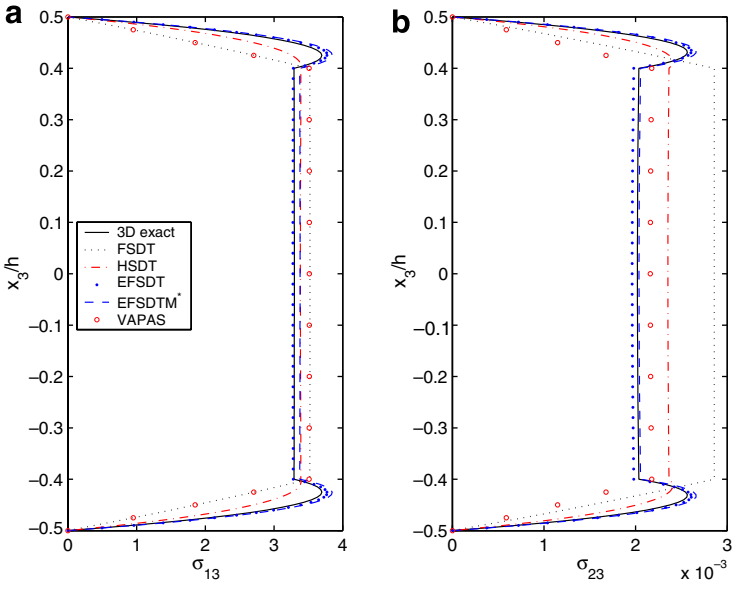

Fig. 12. Transverse shear stresses of a [0.05°/Core(0.05°)/0.05°] sandwich plate with $S = 10$: (a) $\hat{\sigma}_{13}$, (b) $\hat{\sigma}_{23}$.

ory and EFSDT among others capture well the severe zig-zag and kinky variations in both $\hat{u}_1$ and $\hat{\sigma}_{\alpha 3}$. Even for the thick sandwich plate, the results of present theory show an excellent agreement with the exact solutions. To assess the present theory further for sandwich plates, two thick sandwich plates ($S = 10$) with angle-ply face sheets [45°/Core(0.05°)/−45°] and unbalanced cross-ply face sheets [0.05°/Core(0.05°)/90.05°] are considered. The transverse normal stresses for angle-ply and unbalanced cross-ply sandwich plates are shown in Figs. 13 and 14, respectively. In both cases, the present EFSDTM shows far better performance than the FSDT and HSDT in predicting the transverse normal stress. From the results presented above, it can be seen that the present EFSDTM shows the best compromised performance in terms of accuracy and efficiency. In the case the present theory fails to predict accurate through-the-thickness variations of transverse stresses, three-dimensional layerwise models (including transverse normal effect), which are computationally intensive, should be used, as reported in literature (Carrera, 1999b; Icardi, 2001).

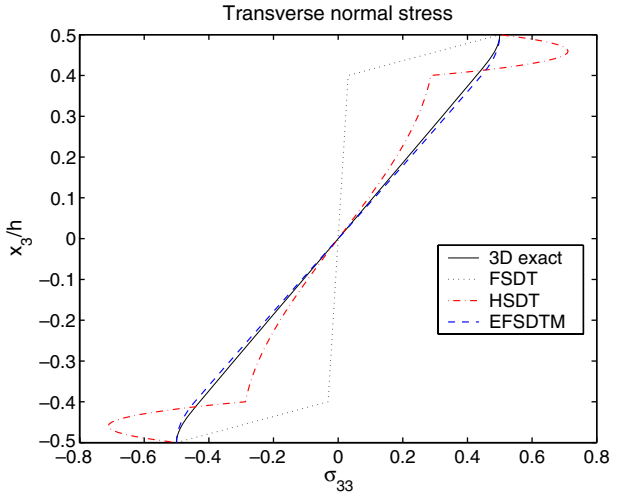

Fig. 13. Transverse normal stress $\hat{\sigma}_{33}$ of a [45°/Core(0.05°)/−45°] sandwich plate with $S = 10$.

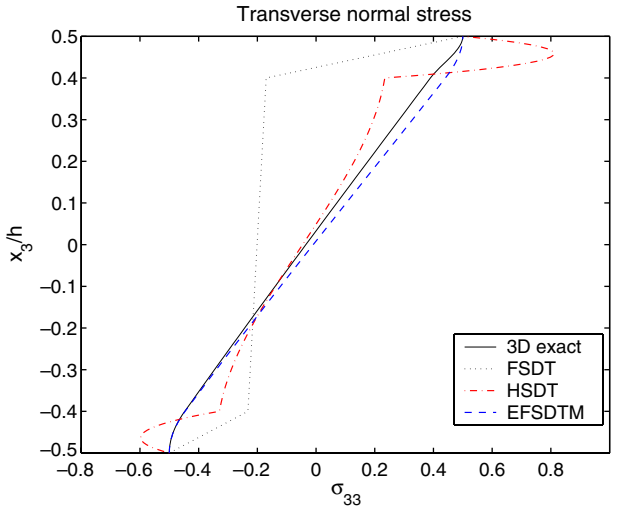

Fig. 14. Transverse normal stress $\hat{\sigma}_{33}$ of a [0.05°/Core(0.05°)/90.05°] sandwich plate with $S = 10$.

6. Conclusions

An enhanced first-order shear deformation theory based on the mixed variational theorem (EFSDTM) has been developed. As compared to the previous EFSDT (Kim, 2004; Kim and Cho, 2005, 2006), it has been improved that the present theory can be able to express nonzero lateral conditions of the transverse shear stresses at top and bottom surfaces and satisfy the transverse normal stress equilibrium exactly. By obtaining the transverse shear stresses based on an EFHOPT (Cho and Parmerter, 1992, 1993), the mixed variational formulation embraces them as the classical FSDT, which renders the present theory (EFSDTM). Relationships between an EHOPT and the classical FSDT were systematically derived via the mixed variational theorem and the least-square approximation of difference between in-plane stresses including the transverse normal stress effect.

The present theory was used to explore the static behavior of laminated and sandwich plates. Comparisons of displacements and stresses for laminated and sandwich plates were made with the available data reported in literature and three-dimensional exact solutions. It was shown that the transverse normal stress effect should be considered in predicting the in-plane stresses when the Poisson effect is dominant. The accuracy and efficiency of the present EFSDTM were demonstrated via various examples. Although the present theory is as simple as an equivalent single layer theory (e.g., FSDT), the recovered results, such as in-plane displacements and transverse stresses, have excellent accuracy as compared to the higher-order shear deformation theories (HSDT and LCW).

Acknowledgements

The authors wish to thank Prof. Wenbin Yu at Utah State University for providing the VAPAS graphical data.

Appendix A. Derivation of predetermined constants for any strain fields

The in-plane strains based on the FSDT displacements given in Eq. (35) can be expressed by

$$\overline{\mathscr{E}}_e = \overline{\mathscr{E}}_0 + x_3\overline{\mathscr{K}}_0 + x_3 I_e \overline{\mathscr{K}}_\gamma, \tag{A.1}$$

where

$$\overline{\mathscr{E}}_0 = \lfloor\, \bar{u}^0_{1,1} \quad \bar{u}^0_{2,2} \quad (\bar{u}^0_{1,2} + \bar{u}^0_{2,1}) \,\rfloor^{\mathrm{T}}, \qquad \overline{\mathscr{K}}_0 = -\lfloor\, \bar{u}^0_{3,11} \quad \bar{u}^0_{3,22} \quad 2\bar{u}_{3,12} \,\rfloor^{\mathrm{T}}, \tag{A.2}$$

$$\overline{\mathscr{K}}_\gamma = \lfloor\, \bar{\gamma}_{31,1} \quad \bar{\gamma}_{32,2} \quad \bar{\gamma}_{31,2} \quad \bar{\gamma}_{32,1} \,\rfloor^{\mathrm{T}}, \tag{A.3}$$

and

$$I_e = \begin{bmatrix} 1 & 0 & 0 & 0 \\ 0 & 1 & 0 & 0 \\ 0 & 0 & 1 & 1 \end{bmatrix}. \tag{A.4}$$

The stress resultants' vector using Eq. (A.1) is given by

$$\widetilde{\overline{N}} = \left\langle \bar{\sigma}^{\mathrm{2D}}_{\alpha\beta} \right\rangle = A\overline{\mathscr{E}}_0 + B\overline{\mathscr{K}}_0 + BI_e\overline{\mathscr{K}}_\gamma, \tag{A.5}$$

in which

$$\widetilde{\overline{N}} = \lfloor\, \overline{N}_{11} \quad \overline{N}_{22} \quad \overline{N}_{12} \,\rfloor^{\mathrm{T}}, \qquad A = \langle \widetilde{Q} \rangle, \qquad B = \langle x_3 \widetilde{Q} \rangle, \tag{A.6}$$

where $\widetilde{Q}$ is 3×3 matrix corresponding to $Q_{\alpha\beta\gamma\omega}$ given in Eq. (9), and A and B are 3×3 matrices that are the well-known transformed reduced stiffness matrices in the classical FSDT (Reddy, 1997).

The in-plane strains based on the recovered displacements given in Eq. (60) are written by

$$\mathscr{E}_e = \overline{\mathscr{E}}_0 + x_3\overline{\mathscr{K}}_0 + \widetilde{\Phi}^*(x_3)\overline{\mathscr{K}}_\gamma + \widetilde{\Lambda}^{p*}(x_3)\mathscr{K}^+_\gamma + \widetilde{\Lambda}^{m*}(x_3)\mathscr{K}^-_\gamma - \tilde{c}, \tag{A.7}$$

where

$$\mathscr{K}_{\gamma}^{\pm} = \lfloor\, \gamma_{31,1}^{\pm} \quad \gamma_{32,2}^{\pm} \quad \gamma_{31,2}^{\pm} \quad \gamma_{32,1}^{\pm} \,\rfloor^{\mathrm{T}}, \qquad \tilde{c} = \lfloor\, c_{1,1} \quad c_{2,2} \quad (c_{1,2}+c_{2,1}) \,\rfloor^{\mathrm{T}}, \tag{A.8}$$

$$\widetilde{\Phi}^{*}(x_3) = \begin{bmatrix} \Phi_{11}^{*}(x_3) & 0 & 0 & \Phi_{12}^{*}(x_3) \\ 0 & \Phi_{22}^{*}(x_3) & \Phi_{21}^{*}(x_3) & 0 \\ \Phi_{21}^{*}(x_3) & \Phi_{12}^{*}(x_3) & \Phi_{11}^{*}(x_3) & \Phi_{12}^{*}(x_3) \end{bmatrix}, \tag{A.9}$$

$$\widetilde{\Lambda}^{(p*,m*)}(x_3) = \begin{bmatrix} \Lambda_{11}^{(p*,m*)}(x_3) & 0 & 0 & \Lambda_{12}^{(p*,m*)}(x_3) \\ 0 & \Lambda_{22}^{(p*,m*)}(x_3) & \Lambda_{21}^{(p*,m*)}(x_3) & 0 \\ \Lambda_{21}^{(p*,m*)}(x_3) & \Lambda_{12}^{(p*,m*)}(x_3) & \Lambda_{11}^{(p*,m*)}(x_3) & \Lambda_{12}^{(p*,m*)}(x_3) \end{bmatrix}. \tag{A.10}$$

In order to calculate the three-dimensional in-plane stresses, it is needed to express the transverse normal stress in the vector form. Furthermore, it should be expressed in terms of the two-dimensional in-plane strains to obtain arbitrary functions c_α for any strain fields. From Eqs. (33), (44) and (65), the recovered transverse normal stress can be rewritten by

$$\sigma_{33}^{\mathrm{e}} = -\left(\widetilde{\Phi}^{t}(x_3)\overline{\mathscr{K}}_{\gamma} + \widetilde{\Lambda}^{tp}(x_3)\mathscr{K}_{\gamma}^{+} + \widetilde{\Lambda}^{tm}(x_3)\mathscr{K}_{\gamma}^{-} \right) - q^{-}, \tag{A.11}$$

in which

$$\widetilde{\Phi}^{t}(x_3) = \lfloor\, \Phi_{11}^{t}(x_3) \quad \Phi_{22}^{t}(x_3) \quad \Phi_{21}^{t}(x_3) \quad \Phi_{12}^{t}(x_3) \,\rfloor, \tag{A.12}$$

$$\widetilde{\Lambda}^{(tp,tm)}(x_3) = \lfloor\, \Lambda_{11}^{(tp,tm)}(x_3) \quad \Lambda_{22}^{(tp,tm)}(x_3) \quad \Lambda_{21}^{(tp,tm)}(x_3) \quad \Lambda_{12}^{(tp,tm)}(x_3) \,\rfloor, \tag{A.13}$$

where

$$\Phi_{\alpha\mu}^{t}(x_3) = \int_{-\frac{h}{2}}^{x_3} C_{\alpha 3\beta 3}\mathscr{A}_{\beta\lambda}(x_3)\widetilde{A}_{\lambda 3\gamma 3}^{-1}\widehat{A}_{\gamma 3\mu 3}\,\mathrm{d}x_3, \tag{A.14}$$

$$\Lambda_{\alpha\mu}^{tp}(x_3) = \int_{-\frac{h}{2}}^{x_3} C_{\alpha 3\beta 3}\left\{ \mathscr{B}_{\beta\mu}(x_3) - \mathscr{A}_{\beta\lambda}(x_3)\widetilde{A}_{\lambda 3\gamma 3}^{-1}\widetilde{B}_{\gamma 3\mu 3} \right\}\mathrm{d}x_3, \tag{A.15}$$

$$\Lambda_{\alpha\mu}^{tm}(x_3) = \int_{-\frac{h}{2}}^{x_3} C_{\alpha 3\beta 3}\left\{ \mathscr{C}_{\beta\mu}(x_3) - \mathscr{A}_{\beta\lambda}(x_3)\widetilde{A}_{\lambda 3\gamma 3}^{-1}\widetilde{D}_{\gamma 3\mu 3} \right\}\mathrm{d}x_3. \tag{A.16}$$

From Eqs. (A.7) and (A.11), the stress resultants' vector is expressed by

$$\widetilde{N} = \left\langle \sigma_{\alpha\beta}^{\mathrm{2D}} + \overline{C}_{\alpha\beta 33}\sigma_{33}^{\mathrm{e}} \right\rangle = A\overline{\mathscr{E}}_0 + B\overline{\mathscr{K}}_0 + (E-E^{t})\overline{\mathscr{K}}_{\gamma} + (F^{p}-F^{tp})\mathscr{K}_{\gamma}^{+} + (F^{m}-F^{tm})\mathscr{K}_{\gamma}^{-} - A\tilde{c} - \langle \widetilde{C}_{et} \rangle q^{-}, \tag{A.17}$$

in which

$$\widetilde{N} = \lfloor\, N_{11} \quad N_{22} \quad N_{12} \,\rfloor^{\mathrm{T}}, \qquad \widetilde{C}_{et} = \lfloor\, \overline{C}_{1133} \quad \overline{C}_{2233} \quad \overline{C}_{1233} \,\rfloor^{\mathrm{T}}, \tag{A.18}$$

$$E = \langle \widetilde{Q}\widetilde{\Phi}^{*} \rangle, \qquad F^{(p,m)} = \langle \widetilde{Q}\widetilde{\Lambda}^{(p*,m*)} \rangle, \tag{A.19}$$

$$E^{t} = \langle \widetilde{C}_{et}\widetilde{\Phi}^{t} \rangle, \qquad F^{(tp,tm)} = \langle \widetilde{C}_{et}\widetilde{\Lambda}^{(tp,tm)} \rangle. \tag{A.20}$$

The difference between in-plane stress resultants presented in Eqs. (A.5) and (A.17) can be expressed as

$$\widetilde{N} - \widetilde{\overline{N}} = (E - BI_e - E^{t})\overline{\mathscr{K}}_{\gamma} + (F^{p}-F^{tp})\mathscr{K}_{\gamma}^{+} + (F^{m}-F^{tm})\mathscr{K}_{\gamma}^{-} - A\tilde{c} - \langle \widetilde{C}_{et} \rangle q^{-} = 0. \tag{A.21}$$

Using Eq. (A.21), the correction vector, $\tilde{c}$, can be obtained by

$$\tilde{c} = \tilde{c}^{*}\overline{\mathscr{K}}_{\gamma} + \tilde{c}^{p}\mathscr{K}_{\gamma}^{+} + \tilde{c}^{m}\mathscr{K}_{\gamma}^{-} - \tilde{c}^{q}q^{-}, \tag{A.22}$$

where

$$\tilde{c}^{*} = A^{-1}(E - BI_e - E^{t}), \tag{A.23}$$

$$\tilde{c}^{(p,m)} = A^{-1}\{F^{(p,m)} - F^{(tp,tm)}\}, \tag{A.24}$$

$$\tilde{c}^{q} = A^{-1}\langle \widetilde{C}_{et} \rangle, \tag{A.25}$$

in which $\tilde{c}^{*}$ and $\tilde{c}^{(p,m)}$ are constant 3×4 matrices, and $\tilde{c}^{q}$ is a constant 3×1 vector.

At this point, it should noted that the last term presented in correction vector to the two-dimensional in-plane strains, Eq. (A.22), is not used in predicting the in-plane displacements, u_α, since the last term, $\tilde{c}^{q}q^{-}$, reflects the transverse normal strain. Therefore, the correction functions to displacements c_α are calculated as follows:

$$c_\alpha(x_\alpha) = c^{*}_{\alpha\beta}\bar{\gamma}_{\beta 3}(x_\alpha) + c^{p}_{\alpha\beta}\gamma^{+}_{\beta 3}(x_\alpha) + c^{m}_{\alpha\beta}\gamma^{-}_{\beta 3}(x_\alpha), \tag{A.26}$$

where $c^{*}_{\alpha\beta}$ and $c^{p,m}_{\alpha\beta}$ can be obtained from Eqs. (A.23) and (A.24), respectively, by assuming that

$$\tilde{c}^{(*,p,m)} = \begin{bmatrix} \underline{c_{11}^{(*,p,m)}} & 0 & 0 & \underline{c_{12}^{(*,p,m)}} \\ 0 & \underline{c_{22}^{(*,p,m)}} & \underline{c_{21}^{(*,p,m)}} & 0 \\ c_{21}^{(*,p,m)} & c_{12}^{(*,p,m)} & c_{11}^{(*,p,m)} & c_{12}^{(*,p,m)} \end{bmatrix}. \tag{A.27}$$

In this study, the underline terms given Eq. (A.27) are selected since they reflects the in-plane normal strains.

References

Carrera, E., 1998. Evaluation of layerwise mixed theories for laminated plates analysis. AIAA Journal 36 (5), 830–839.

Carrera, E., 1999a. A study of transverse normal stress effect on vibration of multilayered plates and shells. Journal of Sound and Vibration 225, 803–829.

Carrera, E., 1999b. Transverse normal stress effects in multilayered plates. Journal of Applied Mechanics 66 (4), 1004–1012.

Carrera, E., 2003. Historical review of zig-zag theories for multilayered plates and shells. Applied Mechanics Review 56, 287–308.

Cho, M., Choi, Y.J., 2001. A new postprocessing method for laminated composites of general lamination configurations. Composite Structures 54, 397–406.

Cho, M., Kim, J.H., 1996a. Postprocess method using displacement field of higher order laminated composite plate theory. AIAA Journal 34, 362–368.

Cho, M., Kim, J.-S., 1996b. Four-noded finite element post-process method using a displacement filed of higher order laminated composite plate theory. Computers and Structures 61, 283–290.

Cho, M., Kim, J.-S., 1997. Improved Mindlin plate stress analysis for laminated composites in finite element method. AIAA Journal 35, 587–590.

Cho, M., Parmerter, R.R., 1992. An efficient higher order plate theory for laminated composites. Composite Structures 20, 113–123.

Cho, M., Parmerter, R.R., 1993. Efficient higher order composite plate theory for general lamination configurations. AIAA Journal 31, 1299–1306.

DiSciuva, M., 1986. Vibration and buckling of simply supported thick multilayered orthotropic plates: an evaluation of a new displacement model. Journal of Sound and Vibration 105, 425–442.

Gregory, R.D., Wan, F.Y.M., 1985. On plate theories and Saint-Venant's principle. International Journal of Solids and Structures 21 (10), 1005–1024.

Icardi, U., 2001. Higher-order zig-zag model for analysis of thick composite beams with inclusion of transverse normal stress and sublaminates approximations. Composites: Part B 32, 343–354.

Icardi, U., Zardo, G., 2005. c^{0} plate element for delamination damage analysis, based on a zig-zag model and strain energy updating. International Journal of Impact Engineering 31, 579–606.

Kant, T., 1982. Numerical analysis of thick plates. Computer Methods in Applied Mechanics and Engineering 31, 1–18.

Kapania, R.K., Raciti, S., 1989. Recent advances in analysis of laminated beams and plates. AIAA Journal 27, 923–934.

Kim, J.-S., 2004. Reconstruction of first-order shear deformation theory for laminated and sandwich shells. AIAA Journal 42, 1685–1697.

Kim, J.-S., Cho, M., 1998. Matching technique of postprocess method using displacement fields of higher order plate theories. Composite Structures 43, 71–78.

Kim, J.-S., Cho, M., 2005. Enhanced first-order shear deformation theory for laminated and sandwich plates. Journal of Applied Mechanics 72, 809–817.

Kim, J.-S., Cho, M., 2006. Enhanced modeling of laminated and sandwich plates via strain energy transformation. Composites Science and Technology 66, 1575–1587.

Knight Jr., N.F., Qi, Y., 1997. Restatement of first-order shear-deformation theory for laminated plates. International Journal of Solids and Structures 34, 481–492.

Lo, K.H., Christensen, R.M., Wu, F.M., 1977. A higher-order theory of plate deformation. Part 2: Laminated plates. Journal of Applied Mechanics 44, 669–676.

Mindlin, R.D., 1951. Influence of rotary inertia and shear on flexural motions of isotropic, elastic plates. Journal of Applied Mechanics 18, 31–38.

Noor, A.K., Burton, W.S., 1989. Assessment of shear deformation theories for multilayered composite plates. Applied Mechanics Reviews 42, 1–13.

Noor, A.K., Burton, W.S., 1990. Stress and free vibration analysis of multilayered composite plates. Composite Structures 14, 233–265.

Pagano, N.J., 1970. Influence of shear coupling in cylindrical bending of anisotropic laminates. Journal of Composite Materials 4, 330–343.

Pandya, B.N., Kant, T., 1988. Finite element stress analysis of laminated composite plates using higher order displacement model. Composites Science and Technology 32, 137–155.

Reddy, J.N., 1984. A simple higher-order theory for laminated composite plates. Journal of Applied Mechanics 51, 745–752.

Reddy, J.N., 1987. A generalization of two-dimensional theories of laminated plates. Communication in Numerical Methods in Engineering 3, 173–180.

Reddy, J.N., 1997. Mechanics of laminated composite plates, theory, and analysis. CRC Press.

Reddy, J.N., Robbins Jr., D.H., 1994. Theories and computational models for composite laminates. Applied Mechanics Review 47, 147–169.

Reissner, E., 1945. The effect of transverse shear deformation on the bending of elastic plates. Journal of Applied Mechanics 12, 69–77.

Reissner, E., 1950. On a variational theorem in elasticity. Journal of Mathematics and Physics 29, 90–95.

Reissner, E., 1986. On a mixed variational theorem and on shear deformable plate theory. International Journal of Numerical Methods in Engineering 23, 193–198.

Rolfes, R., Rohwer, K., Ballerstaedt, M., 1998. Efficient linear transverse normal stress analysis of layered composite plates. Computers and Structures 68, 643–652.

Sun, C.T., Whitney, J.M., 1973. Shear deformation in heterogeneous anisotropic plates. AIAA Journal 11, 178–183.

Sutyrin, V.G., 1997. Derivation of plate theory accounting asymptotically correct shear deformation. Journal of Applied Mechanics 64, 905–915.

Tarn, J.-Q., Wang, Y.-B., 1997. A refined asymptotic theory and computational model for multilayered composite plates. Computer Methods in Applied Mechanics and Engineering 145, 167–184.

Whitney, J.M., 1972. Stress analysis of thick laminated composites and sandwich plates. Journal of Composite Materials 6, 426–440.

Whitney, J.M., 1973. Shear correction factors for orthotropic laminates under static load. Journal of Applied Mechanics 40, 302–304.

Whitney, J.M., Pagano, N.J., 1970. Shear deformation in heterogeneous anisotropic plates. Journal of Applied Mechanics 37, 1031–1036.

Yu, W., 2005. Mathematical construction of a Reissner–Mindlin plate theory for composite laminates. International Journal of Solids and Structures 42, 6680–6699.

Yu, W., Hodges, D.H., Volovoi, V.V., 2002. Asymptotic construction of Reissner-like composite plate theory with accurate strain recovery. International Journal of Solids and Structures 39, 5185–5203.

Yu, W., Hodges, D.H., Volovoi, V.V., 2003. Asymptotically accurate 3-d recovery from Reissner-like composite plate finite elements. Computers and Structures 81, 399–454.